AAB Dinariyana
Pande Pramudya Deva
I Made Ariana
Dhimas Widhi Handani
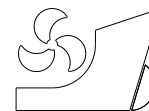
DEVELOPMENT OF MODEL-DRIVEN DECISION SUPPORT SYSTEM TO SCHEDULE UNDERWATER HULL CLEANING

Summary

Maritime industries are constantly searching for a method to enhance ship efficiency, with increasing concern about the environmental impact and rising fuel prices. Marine biofouling is one of the factors that increase ship fuel consumption. However, removing the fouling of the ship requires effort for hull maintenance. Due to the trade-off between conducting maintenance and performance degradation, this study presents the development of a Model-Driven Decision Support System (MD-DSS) to predict the optimum time for underwater hull cleaning for biofouling management. Five stages (sub-models) are employed to develop a DSS, namely: ship resistance estimation, estimation of additional resistance due to biofouling, an iterative-based method for determining the best time to conduct the hull cleaning, and an analysis report. The implemented algorithm was validated by comparing its result with a manually scheduled maintenance date. The DSS is able to determine the best time (date) for maintenance in all given scenarios. By giving two scenarios of different maintenance costs and different fuel prices, the optimisation results produce the same number of maintenances. Within 60 months, four to five hull cleanings are required. It is also found that when the optimal number of maintenances is known, then increasing this number will not have any impact on reducing the hull cleaning costs because the reduction in fouling does not significantly reduce the costs incurred for maintenance. During several trials of the DSS, it is shown that the system can generate maintenance schedules for different time intervals of ship operation within an acceptable time. It takes approximately 52 minutes, 12 minutes, and 5 minutes consecutively to determine the maintenance schedules for ship operation intervals of 5 years, 2.5 years, and 1 year.

Keywords: Biofouling; Decision Support System; Maintenance Scheduling; Underwater Hull Cleaning

1. Introduction

Digitalisation in the maritime industry has become one of the solutions to increase effectiveness and efficiency in the maritime sector, including to support ship operations. Digitalisation will allow ship operators to optimise different aspects of the ship, from ship maintenance and planning/scheduling to ship operation. Three examples of incorporating digitalisation in the maritime industries established by researchers are the optimisation of the maintenance schedule for liquid ring primer in the bilge system using spreadsheet modelling [1], a decision support system for efficient ship operation using an artificial neural network [2], and the development of a weather routing model [3].

In ship operation, fuel oil is the largest of the ship's operational expenses, accounting for almost 50% of the cost of a voyage [4]. The use of fossil fuels also produces greenhouse gases as by-products. With increasing concern about environmental impacts and fuel prices, maritime industry stakeholders are seeking to increase the ship's fuel efficiency. One factor that increases the ship's fuel consumption is the roughness of the ship's hull and propeller, which is caused by accumulated biofouling on the hull [4]. According to the International Maritime Organization (IMO), biofouling has a severe impact both on fuel costs and on emissions of air pollutants and greenhouse gases. Biofouling increases fuel consumption by up to 20% at the end of one year of operation [5]. Biofouling such as heavy slime and heavy calcareous fouling increases the required shaft power by 18% and 76% respectively for destroyer class vessels operating at 15 knots [6].

A model of biofouling development and the effect of hull roughness on the powering requirement have been investigated including the application of biofouling or coating type for specific water condition [7]. The mathematical model based on ITTC-1978 combined with stochastic modelling of the growth of marine organisms is implemented to evaluate the dynamic development of biofouling and its effect on the ship's powering. The developed model is intended to be used to determine the dry-docking schedule of the ship [8]. Biofouling not only affects the roughness of the ship's hull but also has an impact on the surface condition of the ship's propeller. The combination of these two conditions will have an impact on ship performance [9]. One of the attempts made to remove biofouling on ships is to conduct underwater hull cleaning and dry-docking. Implementation of both these hull cleaning methods have time and cost implications. According to Moore Stephens, the dry-docking cost for tankers ranges from 18% to 22% of the 5-year operational costs, which is approximately equal to the cost of 1 year every 5 years [10]. Hull cleaning that is carried out periodically is believed to have an impact on reducing costs due to fuel consumption. Hull cleaning carried out in dry-docking will reduce fuel consumption by 17% compared to 9% when carrying out underwater hull cleaning [11].

Due to the trade-off between increased operational costs and the maintenance cost, the determination of the best time for hull maintenance is key to minimising costs as a result of the growth of fouling, whether from the maintenance cost or operational cost. In order to do so, it is important to analyse a model for predicting an increase in ship resistance and fuel consumption due to fouling. Estimation of ship resistance will be more accurate if detailed and accurate measurements as an initial reference for the surface roughness of the hull can also be carried out. One of them is by taking measurements during dry-docking or before the ship is launched [12]. A Computational Fluid Dynamics based Reynolds-Averaged Navier–Stokes model has been developed to predict the impact of marine coatings and biofouling on ship resistance [13]. A novel technique using multiple cameras to obtain three-dimensional roughness detail has been developed to predict the effect of hull roughness on ship resistance [14]. In addition, the use of numerical simulation and laboratory experiments

up to full-scale in-situ measurements on the ship's hull can improve the estimation of resistance due to the condition of the hull [15].

A decision support tool has been developed for the sustainability of hull surface maintenance. The tool has been implemented in the Baltic Sea region and developed based on several inputs, such as biocide release rate data and fouling growth on coatings under idle conditions. By examining different hull maintenance scenarios, the developed tool enables the simulation of the emission to water and air, the economic cost and the environmental damage cost [16]. In this study, mathematical models are used to do the prediction. The models are then used to develop MD-DSS as a tool to assist personnel in determining the optimum schedule/date for hull cleaning.

The MD-DSS is developed using five stages (sub-models): resistance estimation [17], a simplified time-dependent biofouling growth sub-model [18], hull-propeller matching, an iterative-based optimisation algorithm, and an analysis report. The DSS takes the ship schedule, ship dimensions, engine properties, and propeller properties as input. The first stage or sub-model comprises ship resistance estimation. Basically, there are two ways for the MD-DSS to conduct this stage. First, ship resistance data are obtained from model test results, since the estimation of ship resistance using this method is the most precise. Shipping companies that own ships as well as those with an interest in implementing the MD-DSS will certainly have the data from the model test results. To anticipate the unavailability of model test data, however, this system also provides a ship resistance estimation model. The resistance of merchant ships can generally be predicted using the Guldhammer–Harvald method or the Holtrop–Mennen method. However, in this current developed system, the method used for estimating ship resistance is the Guldhammer–Harvald method, although there are limitations in the use of this method. The range of parameters suitable for the Guldhammer–Harvald method is the value of the Froude number, Fr to 0.33, the value of the block coefficient, C_B in the range of values from 0.55 to 0.85; the length–beam ratio in the range 5.0–8.0 and the length–displacement ratio in the range 4.0–6.0 [19]. In stage two, additional resistance caused by fouling is estimated using the time-dependent biofouling growth model. The third stage aims to find equilibrium between the load and propulsion system using a hull–propeller matching process. The fourth stage is an optimisation done iteratively to determine the number of underwater hull cleanings that gives the minimum cost. The fifth stage aims to provide a report comprising the ship data, engine data, propeller data, voyage schedule, fuel price, and ship schedule, which will be presented along with the output or analysis result (maintenance date, fuel expenses, and maintenance expenses). The DSS process is validated by comparing the result given by the system with a manually calculated combination of dates of hull cleaning. This paper is organised as follows: in section 2, the modelling approach is presented. In section 3, the validation of the optimisation algorithm is elaborated. Finally, section 4 discusses the results of the study together with the assumptions and limitations.

2. Development of DSS for Ship Fouling Maintenance

2.1 General overview

This paper aims to discuss the development of a DSS that can be used by ship operators to determine the best time for conducting hull cleaning. To achieve these goals, five stages (sub-models) are used to develop the DSS, namely, resistance estimation, fouling growth estimation, hull–propeller matching and speed iteration, an iterative-based optimisation algorithm, and an analysis report. The first sub-model is used to estimate resistance in the clean hull condition, the second sub-model is used to estimate the increase of resistance due to hull fouling, the third stage is a hull–propeller matching sub-model to verify the speed of a

ship, the fourth sub-model is used to predict the date for maintenance, and the last sub-model is an analysis report including the cost calculation for the recommended alternative maintenance schedule or date. The developed models are explained in detail in the following sections.

2.2 Resistance estimation sub-model

For estimating total resistance, the sub-model employed the method described in ITTC-1957, as in [17], the Harvald resistance diagram [20], and Mumford formula. The system allowed the user to input measurement data as a source to estimate the ship resistance. The total resistance, R_T, can then be calculated by the following equation:

$$R_T = \frac{1}{2} C_T \rho S V^2 \tag{1}$$

where C_T is the total resistance coefficient, while ρ, S, and V are the water density, wetted surface area and ship speed, respectively. As recommended in ITTC-1978 [21], the total ship resistance coefficient is formulated as

$$C_T = C_F + C_A + C_{AA} + C_R \tag{2}$$

where C_F is the frictional resistance coefficient, C_A is the incremental resistance coefficient, C_{AA} is the air resistance coefficient, and C_R is the residual resistance coefficient. The frictional resistance coefficient in accordance with the ITTC-1957 formula is formulated as

$$C_F = 0.075/(\log R_e - 2)^2 \tag{3}$$

where R_e is the Reynolds number. When Δ is the ship displacement, the incremental resistance coefficient is estimated using the expression described by [17] as follows:

$$1000 \, C_A = 0.5 \log \Delta - 0.1 \, (\log \Delta)^2 \tag{4}$$

The air resistance coefficient value depends on the ship type and size, as shown in Table 1 [17]. The residual resistance coefficient values are taken from Harvald curves for the residual resistance coefficient as a function of the length displacement ratio, prismatic coefficient, and Froude number [17]. For reading the graph, each line is regressed into a polynomial function. The value will then be corrected by B/T correction described in equation (5):

$$C_{R,B/T \neq 2.5} = 0.16(B/T - 2.5)10^{-3} \tag{5}$$

Table 1 C_{AA} value according to ship type and size [17]

Categories	$10^3 \, C_{AA}$
Small tanker	0.07
Handysize tanker	0.07
Handymax tanker	0.07
Panamax tanker	0.05
Aframax tanker	0.05
Suezmax tanker	0.05
VLCC	0.04
Container vessel	0.28 TEU$^{-0.126}$ and ≥ 0.9

Table 2 Antifouling coating performance parameter for each type of fouling [18]

Type	Location	t_0	τ
A	Equatorial	379.4	187.2
	Mediterranean	726.4	129.7
B	Equatorial	271.4	73.11
	Mediterranean	383.5	124.4
C	Equatorial	87	37.08
	Mediterranean	271.9	99.31

The wetted surface area, S, can be estimated by using Mumford's formula described below:

$$S = 1.025 L_{PP} (C_B T + 1.7\ T) \tag{6}$$

where L_{PP} is the length between perpendiculars, C_B is the ship block coefficient, and T is the ship draft.

2.3 Fouling growth sub-model

To predict the increase of ship resistance due to fouling, two models proposed by [18] are used in the DSS. The first prediction model calculates the biofouling growth rate FR and total fouling rating over the period of operation time FR_{tot}, as given in (7) and (8). The second model is used to predict calcareous type fouling surface coverage as a function of time, the effect of which is not considered in the first model. The calcareous type fouling growth rate SC and its accumulated growth rate SC_{tot} during the total operation, as in (9) and (10), are predicted using antifouling coating performance parameters for each type of fouling and constants of logistic curves. The antifouling coating performance parameters are given in Table 2, while the constants of the logistic curves are presented in Table 3 [18].

$$FR = ae^{-\left(\frac{t-t_0}{\tau}\right)^2} \tag{7}$$

$$FR_{tot} = \sum_{i=0}^{n} (\partial FR/\partial t)_i t_i \tag{8}$$

$$SC = (P - p)/\left[1 + \left(e^{b-ct}\right)\right] + d/\left[1 + \left(e^{f-gt}\right)\right] \tag{9}$$

$$SC_{tot} = \sum_{i=0}^{n} (\partial SC/\partial t)_i t_i \tag{10}$$

Table 3 Logistic curve constants [9]

Equatorial		Mediterranean	
P	100	P	0.00517
b	16	b	10
c	0.0407	c	40
d	3.5	d	50
f	10.32	f	32.81
g	0.7759	g	0.04715
p	3.101	p	0

Then, the equivalent sand roughness value is estimated using the regression function, as in

$$k_s(t) = \begin{cases} 0.007143FR_{tot}^2 + 13.36FR_{tot} + 30, & 0 < FR_{tot} \leq 70 \\ 30, & FR_{tot} = 0 \end{cases} \qquad (11)$$

$$k_s(t) = \begin{cases} 2.4669SC_{tot}^2 - 24.84SC_{tot} + 1065.7, & 5 < SC_{tot} \leq 50 \\ 80SC_{tot} + 2000, & 50 < SC_{tot} \leq 100 \end{cases} \qquad (12)$$

It is important to note that if the SC_{tot} is higher than 5% SC, $k_s(t)$ is calculated as in (12).

Several studies have been published for predicting the effect of fouling on ship resistance and powering. Granville similarity law scaling is one of many methods to predict the effect of roughness on the frictional resistance of flat plates of ship lengths by providing the roughness function of fouling [22]. In this fouling growth sub-model, an added resistance diagram (Figure 1) as provided in [23] is used to convert the equivalent sand roughness into the added resistance coefficient due to fouling. The added resistance diagram is converted into a regression function and, by using interpolation, that function is used to convert the ship length, ship speed, and equivalent sand roughness height into the increase of resistance due to fouling. For calculation, this model requires the ship schedule or idle time data, ship speed, and ship length as input.
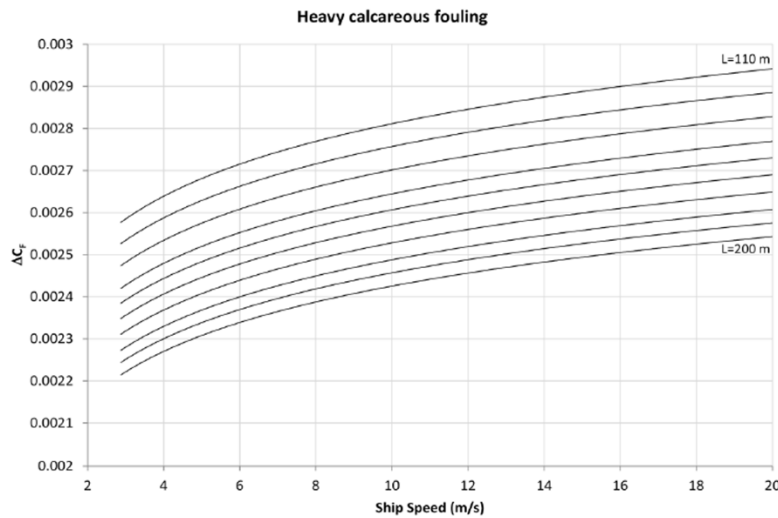
Fig. 1 Added resistance diagram for ships with heavy calcareous fouling [18]

As in [23], similarity law scaling is used to generate the resistance diagram that predicts the roughness effects of coatings and biofouling on ship frictional resistance, shown in the figure below. Each condition represents fouling according to the NSTM rating shown in Table 4.

Table 4 A range of representative coating and fouling conditions [23]

Description of condition	NSTM rating	k_s (µm)
Hydraulically smooth surface	0	0
Typical as applied AF coating	0	30
Deteriorated coating or light slime	10-20	100
Heavy slime	30	300
Small calcareous fouling or weed	40-60	1000
Medium calcareous fouling	70-80	3000
Heavy calcareous fouling	90-100	10000

Therefore, in the case of a ship having an equivalent sand roughness value higher than 1000, after maintenance, it is assumed that the equivalent sand roughness value taken to represent the ship roughness is 1000. Otherwise, if the ship with equivalent sand roughness value below 1000 is cleaned, it is assumed that the cleaning will result in a deteriorated hull condition or equivalent sand roughness value of 100. For dry-docking cleaning, the ship is assumed to return at the initial condition (equivalent sand roughness height value of 30), because it is assumed that in dry-docking cleaning the ship will also be repainted. In the DSS, the user is able to input the increase of ship resistance over time as well as to estimate the growth of fouling.

2.4   Hull–propeller matching sub-model

In this model, hull–propeller matching is used to find the ship speed. Speed equilibrium is maintained between the load or resistance and thrust generated by a propeller at a specific propeller or engine speed and draft condition by utilising iteration. The ship's required thrust and the propeller thrust will be estimated using the following equation. The advance number (J) can be described as

$$J = V_a/(ND) \tag{13}$$

where V_a is the average speed of flow into the propeller, N is the propeller speed, and D is the diameter. The value of V_a can be estimated using the equation described by [17] as follows:

$$V_a = V_s(1 - w) \tag{14}$$

where w is the wake fraction estimated by using British Ship Research Association (BSRA) wake data regression [24] and given as follows:

$$w = -0.0458 + 0.3745C_B^2 + 0.1590\left(B/\nabla^{\frac{1}{3}}\sqrt{\nabla^{\frac{1}{3}}/D}\right) - 0.8636Fr + 1.4773Fr^2 \tag{15}$$

where B is the breadth, ∇ is the volume displacement, and D is the propeller diameter. Using both equations, the advance number can be estimated and used to calculate the value of the propeller thrust coefficient, torque coefficient, and efficiency by employing the propeller open water diagram given in [25] [26].

Dimensional analysis and propeller coefficients describe the relation between different physical variables related to propellers, such as the propeller thrust coefficient [24], torque coefficient, and efficiency, which are described as

$$K_T = T/(\rho N^2 D^4) \tag{16}$$

$$K_Q = Q/(\rho N^2 D^5) \tag{17}$$

$$\eta_o = (JK_T)/(2\pi K_Q) \tag{18}$$

The thrust deduction factor shows the relation between thrust and resistance [24], which can be defined using (19) and estimated as in (20):

$$R = T(1 - t) \tag{19}$$

$$t = -0.2064 + 0.3246C_B^2 - 2.154C_B^2(LCB/L_{PP}) + 0.1705\left(B/\nabla^{\frac{1}{3}}\right) + 0.1504(P/D) \tag{20}$$

where *LCB* is the longitudinal centre of buoyancy and *P/D* is the propeller pitch diameter ratio.

The previous equation is utilised for hull–propeller matching, the result of which is used to estimate the engine power and fuel oil consumption. Starting from total resistance, the estimated engine power is calculated by taking the different components of the total propulsion system efficiencies into account as described below:

$$P = (R * V_s)/\{\eta_o \eta_{RR}[(1-t)/(1-h)]\eta_s \eta_g\} \tag{21}$$

where η_o is the open water propeller efficiency, η_{RR} is the relative rotative efficiency, $(1-t)/(1-h)$ is the hull efficiency, η_s is the shaft efficiency, and η_g is the gearbox efficiency. From the estimation of the engine power, ship speed, and trip duration, the amount of fuel oil consumption (*FOC*) can be predicted using the following equation:

$$FOC = PxTxSFOC \tag{22}$$

where *SFOC* is the specific fuel oil consumption, *T* is the duration of travel, and *P* is the engine power.

2.5   Iterative-based algorithm sub-model

The optimisation algorithm is used to find the optimum date for maintenance. This optimisation is done iteratively by calculating different selected maintenance schedules. The maintenance schedule (time of hull cleaning) that gives the minimum cost will be considered as the best solution. As a limitation to the model, one maintenance per month is the fastest frequency of maintenance that is applicable in the system, although doing multiple maintenances in a short period of time is not practicable. Validation is conducted by comparing the result given by the system to the date selected as the maintenance date. This is to show that the algorithm can predict the maintenance schedule in terms of the practical or operational point of view.

This model is developed by the logic that doing maintenance at the beginning and end of the analysed duration or near to dry-docking is a waste, because doing multiple maintenances in a short period of time serves no purpose. In short, doing multiple maintenances in a short period of time is like cleaning a non-dirty hull, bringing no benefit but inducing a cost. Figure 2 is used to illustrate this statement. The *y* axis represents the cost, and the *x* axis represents the time, while the function used in the figure is *y = 2x*. As there is extra FOC due to fouling growth over time and it only decreases if the ship is cleaned, the lines in the figure will be used to represent extra FOC due to fouling. The red lines represent the ship condition with no maintenance or cleaning, whereas the blue, green, and orange lines represent the cleaned or maintained ship.
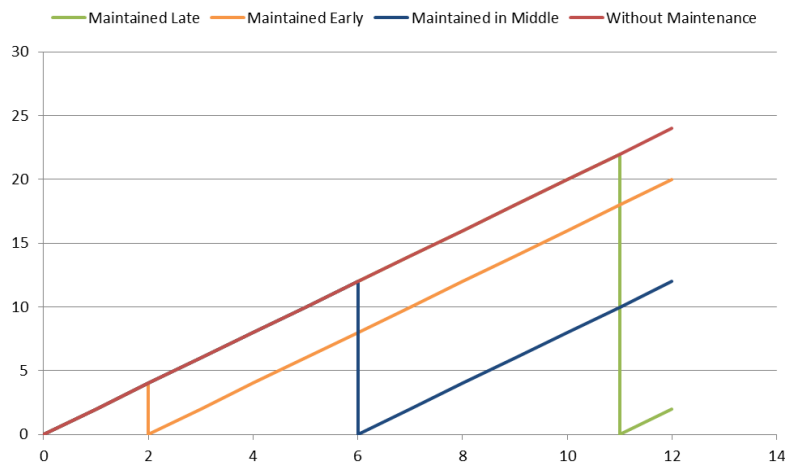
Fig. 2 Illustration of hull cleaning schedule selection

The calculation of the total cost over time in each condition is the total area under the line. The example given shows that the area/cost of a ship without maintenance is 144, while the area/cost of a ship that is maintained at the beginning ($x = 2$) is 104, the area/cost of a ship that is maintained at the end ($x = 11$) is 122, and the area/cost of a ship that is maintained in the middle ($x = 6$) is 72. This illustration shows that doing a hull cleaning in the middle of the duration is more beneficial than at the beginning or at the end or close to another hull cleaning. The maintenance penalty and schedule may cause the optimum time not to be precise in the middle of the duration, so a range in the selection is employed. The maintenance penalty is employed to address practical issues in conducting the hull cleaning. For cleaning soft fouling, the fouling can be removed completely (to be able to see the hull paint), but for cleaning hard fouling, the fouling cannot be removed completely (around 1–2 mm will remain). The equivalent sand roughness height value is taken based on the NSTM standard as well as information gathered from the company. In the case of dry-docking maintenance, a similar approach is used. But the user will need to input the date when the dry-docking is conducted and up to five dry-docking maximums at a time (one analysis is up to 60 months duration). As the maximum combination for dry-docking is small, all combination/cases will be calculated.

2.6 Development of user interface and analysis report

In this model, the fuel price and the maintenance price are set as user input data and are assumed to be constant. This model calculates the fuel cost by multiplying the extra fuel oil consumption due to fouling with the fuel price, and also calculates the maintenance cost by multiplying the number of maintenances with the maintenance price. A DSS user interface (UI) was developed using the Excel visual basic application. Several functions will be fitted into the UI, such as input or editing data and analysis. The result of the analysis will also be exported into .pdf file format.

When the user launches the system, he/she can choose between using the existing propeller open water diagram and fouling estimation method or creating/editing a new/existing propeller open water diagram and fouling estimation method. The system also makes it possible for the user to add new ship data and the voyage schedule in addition to available ship data and voyage schedules that have already been inputted as a database in the system. However, the user may also make changes to the data to update the database. For estimation and calculation, the user can select the method of analysis, whether to select manual input of the date of maintenance or to select the best maintenance schedule or the date recommended by the system. The process of creating/editing a new/existing propeller open

water diagram and fouling estimation method is accommodated in the sheet "Graph Input" shown in Figure 3. This figure shows that, through this UI, users can create digital data from KQ, KT, and J open water diagrams. For example, for the KT diagram, the *x*-axis represents the value of J and the *y*-axis is KT. By reading the data from the open water diagram on a certain type of propeller at a certain P/D, the Kt value for each J is inputted into the cell's *x* value and *y* value. This data will be recorded as a database in DSS in tabulated form.

Adding new or editing existing ship data is done using the form shown in Figure 4. Several ship data can be added and saved as the ship database, such as the name, type, the principal dimensions including the block and prismatic coefficient, volume displacement and ship capacity. The user is also able to input the main engine data (power and rpm), propeller data (propeller series/type, diameter, pitch–diameter ratio, number of blades, and area ratio), and gear box data through this UI. The overall UI, giving information on the selected ship and its corresponding schedule, input for cost calculation, the option for the fouling estimation method, and the output cost calculation of the maintenance schedule policy, can be seen in Figure 5. This figure also shows the additional fuel oil consumption in tons after the beginning of the cycle of operation period. As seen in the graph shown on the UI, the fuel oil consumption tends to increase during the ship's operating time up to the period when hull cleaning is carried out.
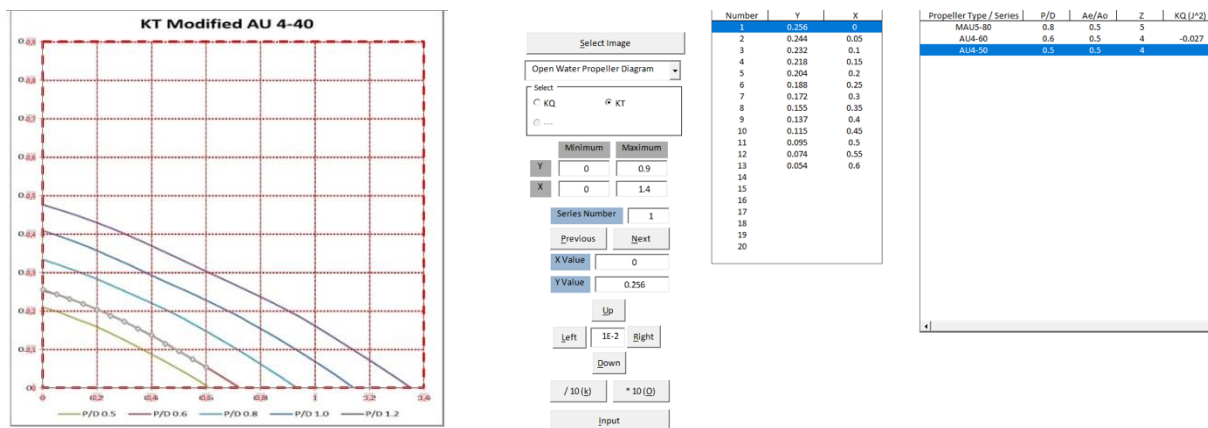
Fig. 3 DSS user interface for graph input
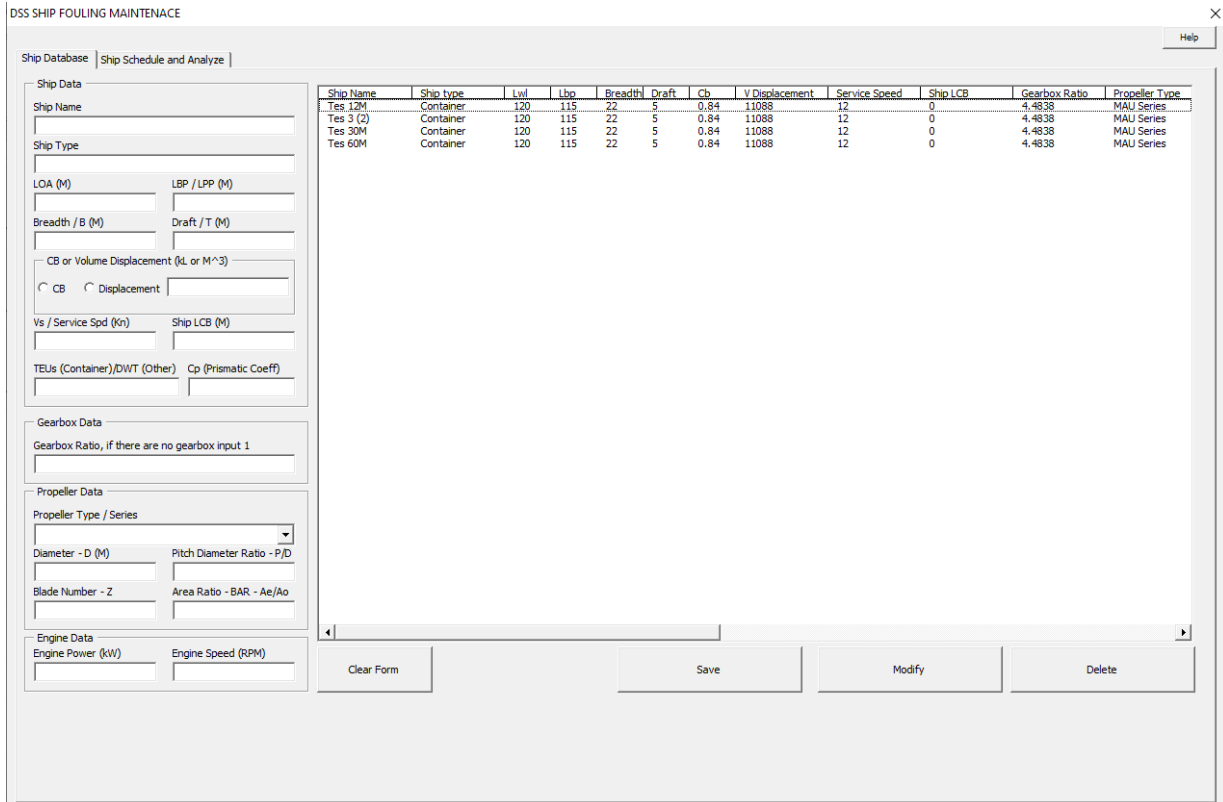
Fig. 4 DSS user interface for ship database
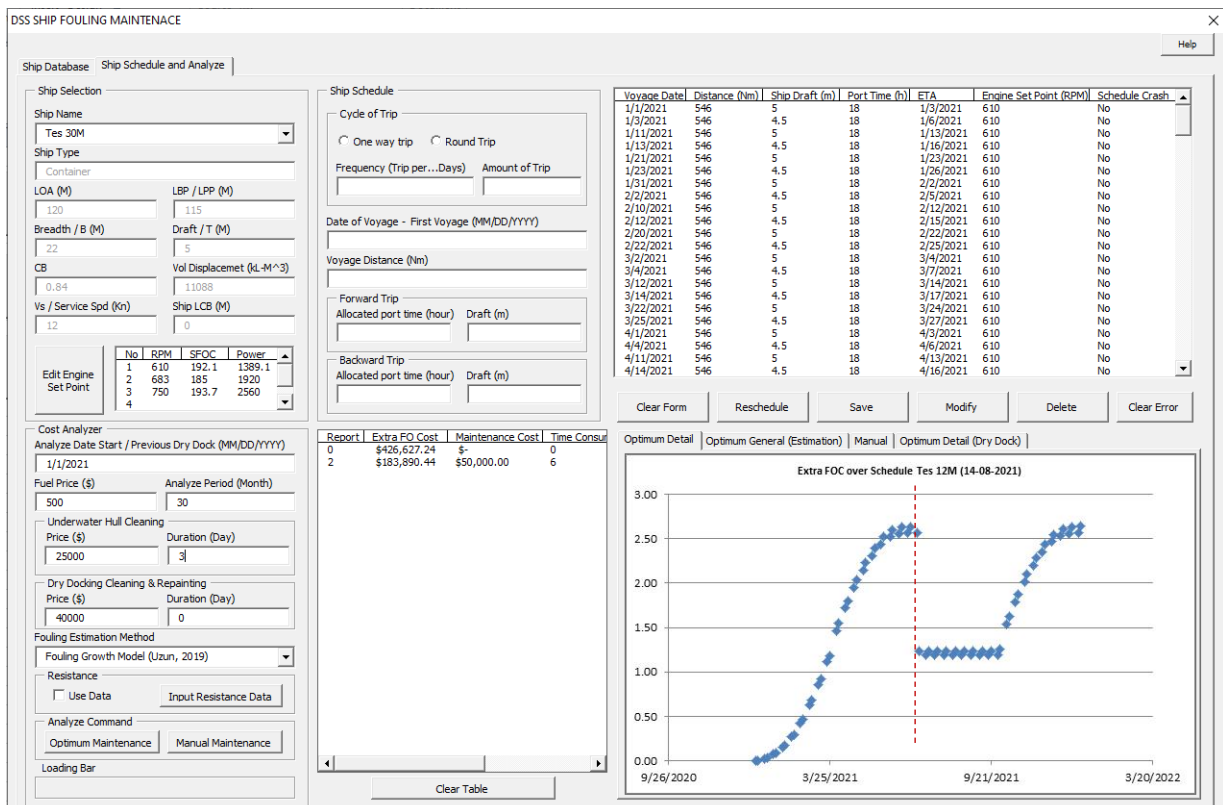
Fig. 5 DSS user interface for ship fouling maintenance

3. Result and Analysis

This section discusses the results of the system, giving several scenarios of the operational time of the ship. The ship data is provided by a shipping company operating in Indonesia. A container ship with a length of 120 m and a capacity of 558 TEUs with a MAU Series type of propeller and diameter of 3.909 m is simulated. Four scenarios of the operational time of the ship are considered. The same route with a duration of 10 days and operational time varying between 60 months, 30 months, 12 months, and 9 months + 1.5 months idle time repeated until 30 months, respectively, is considered as scenario 1 to scenario 4. All scenarios have the same route, Surabaya – Pontianak (546 Nm). The draft is set to be 5 m and 4.5 m, respectively, for the outward trip (Surabaya – Pontianak) and the return trip (Pontianak – Surabaya). The allocated port time is 18 hours for both ports. The outward trip starts every 10 days while the return trip starts directly after the outward trip and port time. The engine is operated at a speed of 610 rpm. Some values are assumed, such as the gearbox efficiency and shaft efficiency (98%), sea water temperature (25ºC), sea water density (1023 kg/m³). All calculations were done on a computer with the specification of Intel i7-7700HQ CPU @ 2.80GHz and 8GB RAM. It took approximately 52 minutes for the DSS to find the optimum underwater hull cleaning time for 5 years making the voyage, 12 minutes for 2.5 years making the voyage, and 5 minutes for 1 year making the voyage.

The selection of the maintenance date was based on the number of planned maintenances within the operational time of the ship considered in each scenario. For a 60-month operational period, the date of the one-time maintenance strategy will be selected between the 1st month and the 60th month. The dates for the two-times maintenance strategy will be selected in months 20 ± 7 and 40 ± 7, where 7 is a range between the midpoints (20 and 40). For the three-maintenance strategy, the maintenance date will be selected in months 15 ± 3, 30 ± 3, and 45 ± 3. The same logic is also used for other scenarios of the operational times. However, the definition of ranges between midpoints may vary according to the operational time of the ship. It is shown that in the same period of ship operation, more maintenance for cleaning the fouling will result in lower additional fuel costs. This is as a result of reducing the roughness of the hull, which means less required engine power for the same ship speed. Table 5 shows the result given by the system for all the scenarios of operating time and number of maintenances.

The algorithm is validated by comparing the results of different combinations of the months selected for conducting maintenance. For one-time maintenance, the results of scenarios 1 to 4 can be seen in Figures 6 to 9, respectively. The vertical axis shows the extra FOC due to hull fouling and the horizontal axis shows the month when maintenance is done. These graphs show that doing cleaning near the beginning and near the end is not the best solution. This condition is given by the four scenarios used in this study. For all scenarios, the best time for conducting maintenance for hull cleaning is located near the mid-point (scenario 1: month 31, scenario 2: month 16, scenario 3: month 7, and scenario 4: month 13) and the best solution is within the ranges of calculation.

Table 5 Result given by the system for all scenarios

Scenario	Number of maintenances	Date (month)	Extra FOC (ton)		Calculation time (minutes)
			Optimised	Not optimised	
1	1	2 Jul 2023 (31)	1681.7	1703.5	35
	2	7 Jul 2022 (19)	1095.6	1067.0	44
		1 Jan 2024 (37)			
	3	1 Apr 2022 (16)	927.1	930.9	90
		2 Jul 2023 (31)			
		4 Oct 2024 (46)			
2	1	4 Jan 2022 (16)	448.03	456.14	8
	2	2 Nov 2021 (11)	372.83	372.83	10
		5 Sep 2022 (21)			
	3	1 Aug 2021 (8)	333.22	340.33	39
		1 Apr 2022 (16)			
		4 Nov 2022 (23)			
3	1	2 Jul 2021 (7)	113.78	11.82	1
	2	3 May 2021 (5)	86.11	89.40	1
		3 Sep 2021 (9)			
	3	3 Apr 2021 (4)	75.59	74.83	1
		2 Jul 2021 (7)			
		3 Oct 2021 (10)			
4	1	7 Feb 2022 (13)	418.49	423.99	4
	2	9 Nov 2021 (10)	323.43	327.35	9
		15 Sep 2022 (19)			
	3	9 Nov 2021 (10)	293.05	299.78	32
		1 Apr 2022 (15)			
		15 Sep 2022 (19)			
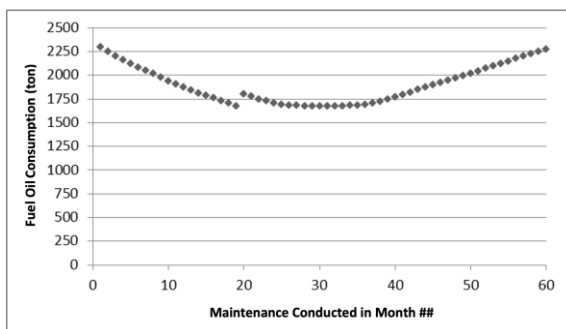
Fig. 6 FOC over time for hull cleaning (scenario 1)
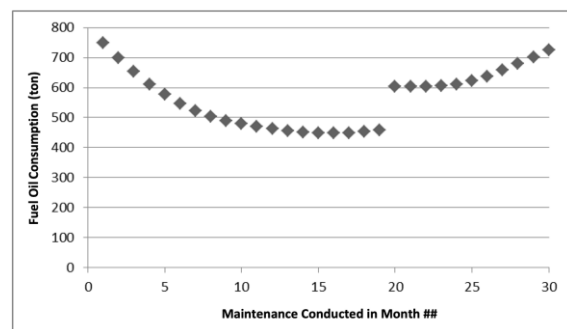
Fig. 7 FOC over time for hull cleaning (scenario 2)
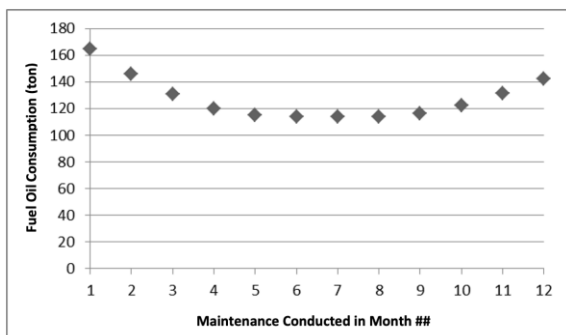
Fig. 8 FOC over time for hull cleaning (scenario 3)
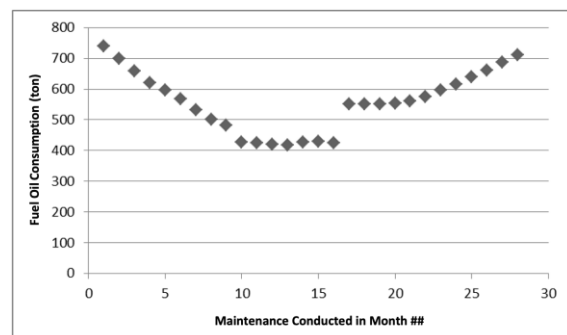
Fig. 9 FOC over time for hull cleaning (scenario 4)

For the two-times maintenance, the result of a manually calculated maintenance date selected is presented partially in the heat map from Figures 10 to 13 for scenarios 1 to 4, respectively. The vertical and horizontal axes represent the months to conduct the first and the second maintenance. The lighter the colour in the pixel/block, the more optimum (lower cost

or FOC) it is in comparison to the darker colour. The result shows that the best decision for conducting hull cleaning is near the midpoint, and the optimum solution is within the ranges of calculation. These indicate the same effect or phenomenon as the one-time maintenance.

Fig. 10 Heat map of FOC over time for hull cleaning (scenario 1)
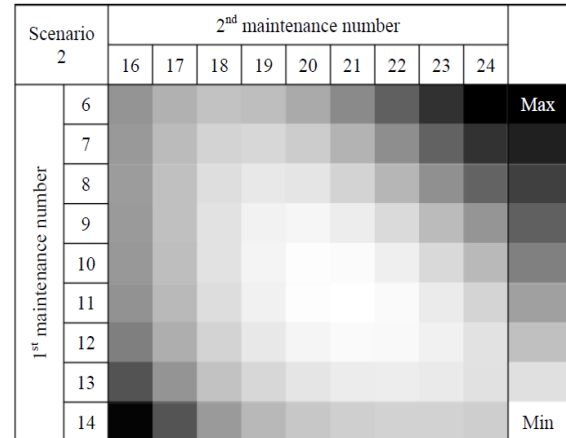
Fig. 11 Heat map of FOC over time for hull cleaning (scenario 2)
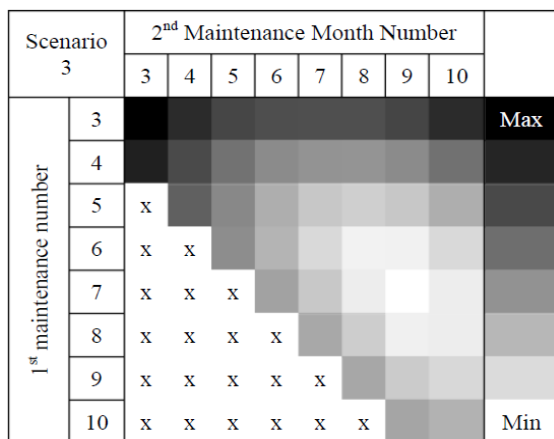
Fig. 12 Heat map of FOC over time for hull cleaning (scenario 3)
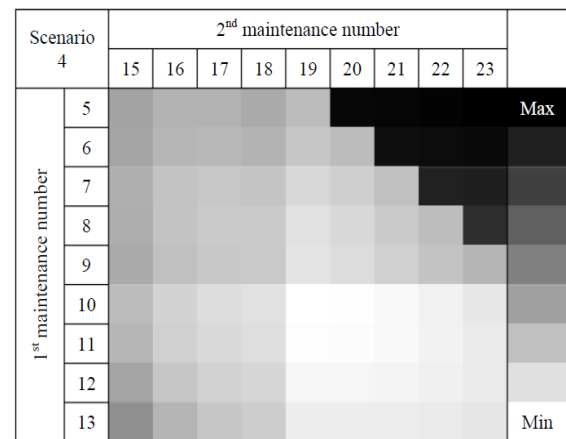
Fig. 13 Heat map of FOC over time for hull cleaning (scenario 4)

The findings from the results of one-time and two-times maintenance show that the graph has two local minima. This is because there are two types of penalty used in the model. This causes a break or jump of value after month 19 in scenarios 1 and 2 and after month 16 in scenario 4. For two-times maintenance, this is shown by the jump in value if the first maintenance in scenario 1 is later than month 19. This also happens in scenario 1 if the range or delay between the first and second maintenance is equal to or higher than 19 months. These findings show that after specific months the ship will have calcareous fouling and will have a higher penalty which results in a higher cost.

It is important to know that the maintenance or hull cleaning has to be conducted within a certain period of ship operation. This section discusses two conditions, with different hull cleaning costs and different fuel prices. Figure 14 shows the number of maintenances during 60 months with two different maintenance or hull cleaning costs, US$ 25,000 and US$ 50,000. When the cost is US$ 25,000, hull cleaning is conducted five times and when the hull cleaning cost is US$ 50,000, the hull cleaning is conducted four times. Figure 15 shows that the number of hull cleanings is five when the fuel price is US$ 600 and four when the fuel

price is US$ 400. All scenarios are conducted for a hull cleaning cost which is US$ 25,000. It can be concluded that the fuel price and maintenance cost do affect the optimum number of maintenances during 60 months of the ship operation. When the optimal number of maintenances is known, then increasing this number will not reduce the hull cleaning costs because the reduction in fouling does not significantly reduce the costs incurred for maintenance.
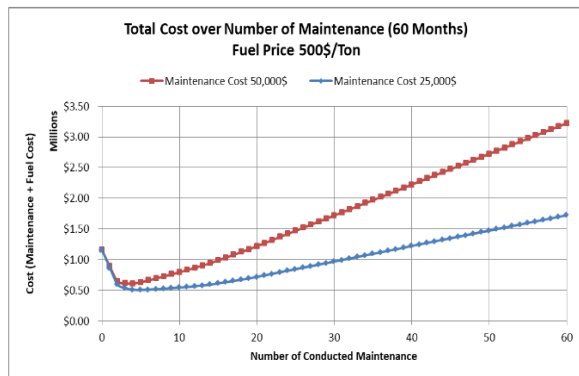
Fig. 14 Total cost for number of hull cleanings during 60 months for different hull cleaning costs
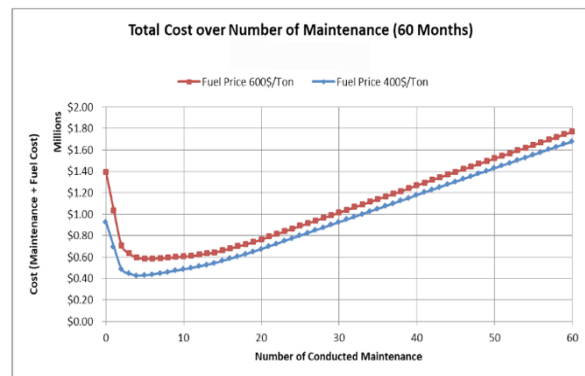
Fig. 15 Total cost for number of hull cleanings during 60 months for different fuel prices

4. Discussion and Conclusions

A model-driven DSS has been developed to help the ship operator to schedule underwater hull cleaning and to define the number of hull cleanings during a certain period of time. The DSS was developed by implementing five sub-models. The first sub-model was developed based on ITTC 1957, the Harvald resistance diagram, and Mumford formula, as that model is sufficient to be used to estimate ship resistance. The alternative of using measurement data was also provided, as using measurement data is more accurate than using the estimation method. The second sub-model was developed based on a time-dependent biofouling growth model. The DSS has been developed only for self-polishing coating type antifouling, which means this model cannot be applied to ships using other types of antifouling. Although in the DSS there was an alternative of using user measurement or trend data of increasing resistance over time, it still has the limitation that it cannot be used in every ship or condition.

The third sub-model was developed based on the hull–propeller matching process. It uses iteration (Newton–Raphson method/ Excel Goal Seek) for searching for the matching condition. The iteration itself cannot exactly match the load thrust and propeller thrust, but the average deviation of 10^{-8} % is small enough to be ignored. The fourth sub-model is the optimisation algorithm that is used to find the optimum date for maintenance. This optimisation is done iteratively by calculating different selected maintenance schedules. The maintenance schedule (time of hull cleaning) with the minimum cost will be considered the best solution. The result of the fourth model is compared into the manually calculated cases. Comparing both results, the fourth sub-model indeed gives the optimum result among the four scenarios. Although a higher number of maintenances (more than three) is not calculated, it is projected that at a higher number the findings will be similar, due to the recurrence of the optimum solution near the mid-point for one to three maintenances. The fifth sub-model comprises the economic analysis as well as an analysis report on the given input for calculation.

By detailing different scenarios of the ship operation period, it is found that the fuel price and maintenance/hull cleaning cost do affect the optimum number of maintenances

during the operation period. It is also found that once the optimal number of maintenances is known, then increasing that number will not reduce the hull cleaning costs because the reduction in fouling does not significantly reduce the costs incurred for maintenance.

It is important to note that the model is only compared for a specific scenario or specific data input. These scenarios certainly do not exactly represent all possible scenarios or combinations of input data. However, each scenario represents a general condition of ships constantly operating for different durations. In future work, there is still a need to validate the DSS algorithm in different scenarios. The main advantage of the developed DSS is that the model can predict the optimum maintenance date using relatively simple and general data. It can be applied to different types of ship in different operating conditions or routes. This DSS still makes certain assumptions and has some limitations due to the lack of data and the impracticality of modelling the effect on hull maintenance or biofouling. The ideal fouling model should be observed in more detail, as well as the data that show the effect of underwater hull cleaning, whether this is the effect of underwater hull cleaning on the ship surface or roughness or the effect on the antifouling paint efficiency. As in [27], there is a re-fouling rate, which multiplies the rate of fouling growth for each consecutive underwater hull cleaning until a certain threshold is reached. This effect should be taken into consideration in future studies.

ACKNOWLEDGEMENT

REFERENCES

[1]   Artana, K. B., Ishida, K., 2002. Spreadsheet modeling of optimal maintenance schedule for components in wear-out phase. *Reliability Engineering & System Safety*, 77, 81-91. https://doi.org/10.1016/S0951-8320(02)00033-9

[2]   Farag, Y. B. A., 2017. A decision support system for ship's energy efficient operation: based on artificial neural network method. World Maritime University Dissertations, Sweden, 2017.

[3]   Pennino, S., Gaglione, S., Innac, A., Piscopo, V., Scamardella, A., 2020. Development of a New Ship Adaptive Weather Routing Model Based on Seakeeping Analysis and Optimization. *Journal of Marine Science and Engineering*, 8, 270, 1-16. https://doi.org/10.3390/jmse8040270

[4]   Bialystocki, N., Konovessis, D., 2016. On the estimation of ship's fuel consumption and speed curve: A statistical approach, *Journal of Ocean Engineering and Science*, 1(2), 157-166. https://doi.org/10.1016/j.joes.2016.02.001

[5]   Hakim, M. L., Nugroho, B., Nurrohman, M. N., Suastika, I. K., Utama, I. K. A. P., 2019. Investigation of fuel consumption on an operating ship due to biofouling growth and quality of anti-fouling coating. *IOP Conf. Series: Earth and Environmental Science*, 339(1), 1-10. https://doi.org/10.1088/1755-1315/339/1/012037

[6]   Schultz, M. P., Bendick, J. A., Holm, E. R., Hertel, W. M., 2011. Economic impact of biofouling on a naval surface ship. *Journal of Bioadhesion and Biofilm Research*, 27(1), 87-98. https://doi.org/10.1080/08927014.2010.542809

[7]   Suwasono, B., Putra, I. K. A. S., Kristiyono, T. A., Azhar, A., 2021. Adhesive Coating Value Based on the Main Ingredient of Ship Paint. *Brodogradnja*, 72(2), 19-36. https://doi.org/10.21278/brod72202

[8]   Hadžić, N., Gatin, I., Uroić, T., Ložar, V. 2022. Biofouling Dynamic and its Impact on Ship Powering and drydocking. *Ocean Engineering*, 245, 110522. https://doi.org/10.1016/j.oceaneng.2022.110522

[9]   Farkas, A., Degiuli, N., Martić, I., 2021. The Impact of Biofouling on the Propeller Performance. *Ocean Engineering*, 219, 108376. https://doi.org/10.1016/j.oceaneng.2020.108376

[10] Apostolidis, A., Kokarakis, J., Merikas, A. 2012. Modeling the Dry-Docking Cost - The Case of Tankers. *Journal of Ship Production and Design*, 28(3), 134-143. https://doi.org/10.5957/JSPD.28.3.110039

[11] Adland, R., Cariou, P., Jia, H., Wolff, F. C., 2018. The energy efficiency effects of periodic ship hull cleaning. *Journal of Cleaner Production*, 178, 1-13. https://doi.org/10.1016/j.jclepro.2017.12.247

[12] Seok, J., Park, J. C., 2020. A fundamental study on measurement of hull roughness. *Brodogradnja*, 71(1), 59-69. https://doi.org/10.21278/brod71104

[13] Demirel, Y. K., Turan, O., Incecik, A., 2017. Predicting the effect of biofouling on ship resistance using CFD. *Applied ocean research*, 62, 100-118. https://doi.org/10.1016/j.apor.2016.12.003

[14] Utama, I. K. A. P., Nugroho, B., 2018. Biofouling, ship drag, and fuel consumption: A brief overview. *The Journal of Ocean Technology*, 3(2), 43-48.

[15] Hutchins, N., Monty, J. P., Nugroho, B., Ganapathisubramani, B., Utama, I. K. A. P., 2016. Turbulent boundary layers developing over rough surfaces: from the laboratory to full-scale systems. In *20th Australian fluid mechanics conference* (Vol. 1235).

[16] Oliveira, D. R., Lagerström, M., Granhag, L., Werner, S., Larsson, A. I., Ytreberg, E., 2022. A novel tool for cost and emission reduction related to ship underwater hull maintenance. *Journal of Cleaner Production*, 356, 131882. https://doi.org/10.1016/j.jclepro.2022.131882

[17] Kristensen, H. O., Lutzen, M., 2013. Prediction of Resistance and Propulsion Power of Ships. *Technical University of Denmark and University of Southern Denmark*, Denmark.

[18] Uzun, D., Demirel, Y. K., Coraddu, A., Turan, O., 2019. Time-dependent biofouling growth model for predicting the effects of biofouling on ship resistance and powering. *Ocean Engineering*, 191, 106432. https://doi.org/10.1016/j.oceaneng.2019.106432

[19] Birk, L., 2019. Fundamental of Ship Hydrodynamics – Fluid Mechanics, Ship Resistance and Propulsion, 1st Edition, *John Wiley & Sons Ltd*, Padstwo, Cornwall, Great Britain. https://doi.org/10.1002/9781119191575

[20] Harvald, S., 1983. Resistance and Propulsion of Ships, *John Wiley & Sons Ltd*, New York.

[21] ITTC, 1978. 1978 ITTC Performance Prediction Method. International Towing Tank Conference, 1978.

[22] Granville, P. S., 1958. The frictional resistance and turbulent boundary layer of rough surfaces. *Journal of Ship Research*, 2, 52-74. https://doi.org/10.5957/jsr.1958.2.4.52

[23] Demirel, Y. K., 2015. Modelling the Roughness Effects of Marine Coatings and Biofouling on Ship Frictional Resistance, PhD thesis, University of Strathclyde, Glasgow, UK.

[24] Molland, A. F., Turnock, S. R. Hudson, D. A., 2011. Ship Resistance and Propulsion, *Cambridge University Press*, UK. https://doi.org/10.1017/CBO9780511974113

[25] Barnitsas, M. M., Ray, D., Kinley, P., 1981. KT, KQ and efficiency curves for the Wageningen B-series propellers. University of Michigan.

[26] Yazaki, A., Kuramochi, E., Kumasaki, T., 1960. Open water test series with modified au-type four-bladed propeller models. *Journal of Zosen Kiokai*, 1960(108), 99-104. https://doi.org/10.2534/jjasnaoe1952.1960.108_99

[27] Preiser, H. S., Laster, D. R., 1981. On Optimization of Underwater Hull Cleaning for Greater Fuel Economy. *Naval Engineers Journal,* 93, 45-52. https://doi.org/10.1111/j.1559-3584.1981.tb00644.x

Submitted: 04.02.2022.   [ab] AAB Dinariyana, [ab] Pande Pramudya Deva, [ab] I Made Ariana*, [ab] Dhimas Widhi Handani

Accepted: 18.07.2022.   ariana@its.ac.id
[a]Department of Marine Engineering, Institut Teknologi Sepuluh Nopember Kampus ITS Sukolilo, Surabaya, Indonesia 60111
[b]Center of Excellence for Maritime Safety and Marine Installation Institut Teknologi Sepuluh Nopember Kampus ITS Sukolilo, Surabaya, Indonesia 60111